Supporting Information

Natural Abundance High-performance Rechargeable Aluminum/Iodine Battery Based on Conversion Reaction Chemistry

Shunlong Zhang[a,b,c,d⊥], Xiaojian Tan[a⊥], Zhen Meng[a], Huajun Tian[*,a], Fangfang Xu,[c] Wei-Qiang Han[*,a,b,e]

a Ningbo Institute of Materials Technology & Engineering, Chinese Academy of Sciences, Ningbo 315201, China
b School of Physical Science and Technology, Shanghai Tech University, Shanghai 201210, China
c Shanghai Institute of Ceramics, Chinese Academy of Sciences, Shanghai 200050, China
d University of Chinese Academy of Sciences, Beijing 101407, China
e Department of Materials Science and Engineering, Zhejiang University, Hangzhou 310027, China

This file includes characterization of the materials, supplementary tables S1-S2, supplementary figures S1-S20.

Experiments and characterization of the materials

Table S1 A comparison of the characteristics of aluminum metal with those of other metals

Metal	Abundance (ppm)	Price (USD/Kg)	Volumetric Capacity (mAh/ml)	Gravimetric Capacity (mAh/g)	Reduction Potential vs.NHE(V)	Ionic Radius (nm)	Resistivity (uΩ*cm)
Li	17	1500	2062	3861	-3	0.68	8.55
Na	23000	580	1128	1166	-2.7	0.95	4.28
Mg	29000	100	3833	2205	-2.4	0.65	4.45
Al	82000	1.4	8046	2980	-1.7	0.50	2.65

Table S2 The capacity and voltage of AIBs cathode materials reported in literature.

Material	Potential (V)	Capacity (mAh/g)	Energy Density (Wh/kg)	Cycles	Reference
Graphitic-foam	2	~70 at 66 mA/g	~140	>200	1
Ni_3S_2 /Graphene	1	60 at100mA/g	60	100	2
V_2O_5	0.55	130	71.5	5	3
V_2O_5 nanowire	0.5	273	136.5	20	4
VO_2	0.7	70 at 200mA /g	49	100	5
3D Graphitic Foams	1.8	60 at 12A/g	108	40000	6
Carbon paper	1.8	~70	126	100	7
Fluorinated natural graphite	0.65	225 at 60mA/g	~145	40	8
Polythiophene	1.47	30~100 at ~20mA/g	44	100	9
SnS_2	0.68	70 at 200mA/g	47.6	100	10
CuS	1.0	90 at 20mA /g	90	100	11
Zeolite-Templated Carbon (ZTC)	~0.5	178.1 at 100mA /g	89	500	12
TiS_2	0. 75	70 at 5mA /g	52.5	50	13
Mo_6S_8	0. 55	70 at 12mA /g	38.5	50	14
ACC/ PVPI	0.74	180.1 at 42.2mA/g	133	>150	This work

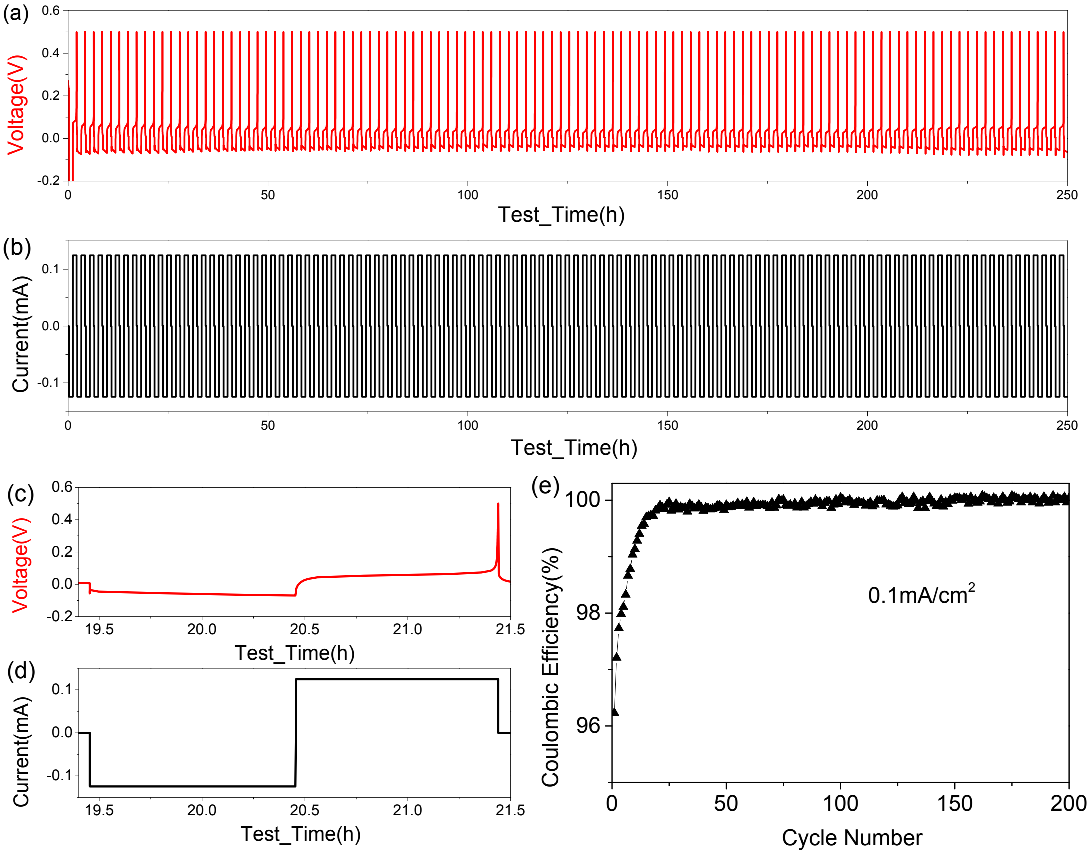

Figure S1. Electrochemical performance of the ionic liquids electrolytes composed of $AlCl_3$/[EMIm]Cl=1.3 in molar ratio. Galvanostatic discharge/charge measurements, Current density: 0.1 mA/cm^2, Discharge time: 1 h. Charge cut-off voltage: 0.5 V. (a) Voltage versus test time profile. (b) Current versus test time profile. (c) A typical curve of Voltage versus test time profile. (d) A typical curve of Current versus test time profile. (e) Coulombic Efficiency for Al deposition/striping. The initial efficiency could reach up to 96.2%, then, after several activation cycles, Coulombic efficiency close to 100% can be achieved.

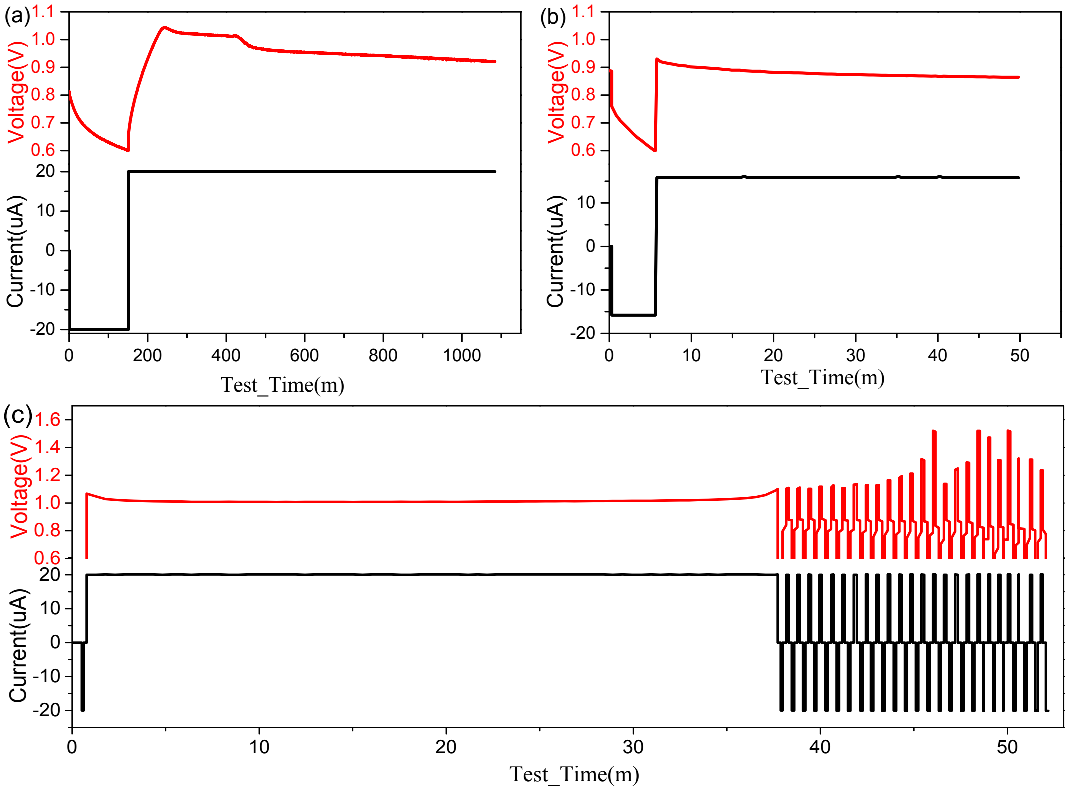

Figure S2. Electrochemical performance measurements of cathode ACC/PVPI in coin cell, because of corrosion caused by electrolytes, the measurements are uncontrollable. (a)-(c) Voltage and Current versus time profiles of different samples.

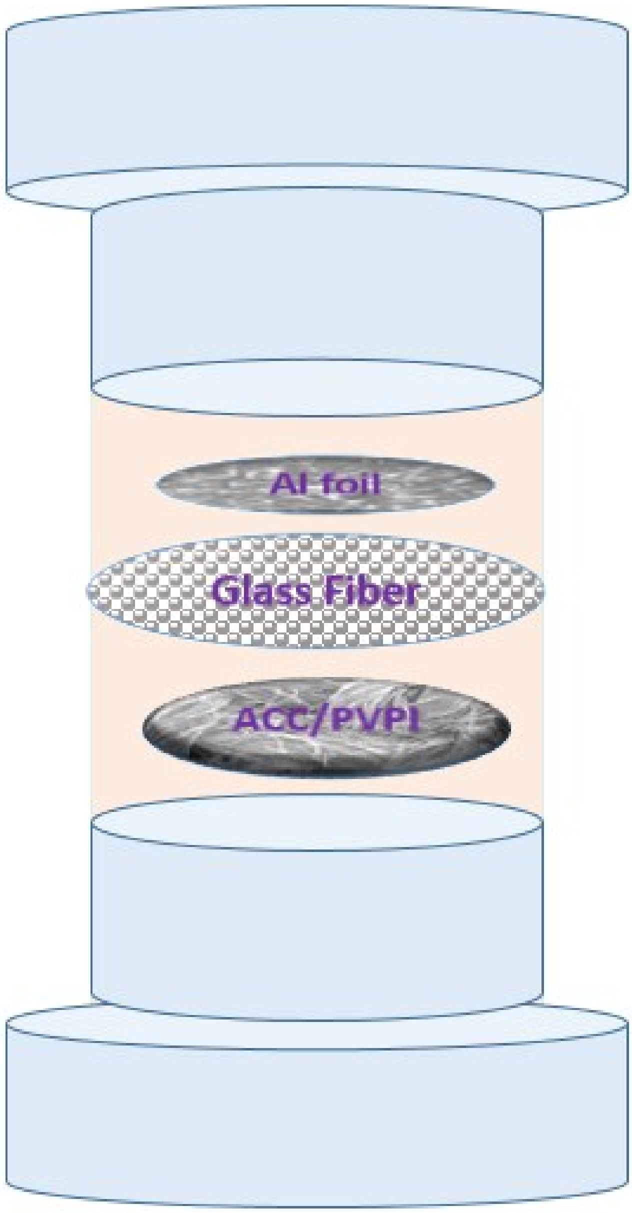

Figure S3. A schematic illustration of Al/I_2 battery in Swagelok cell.

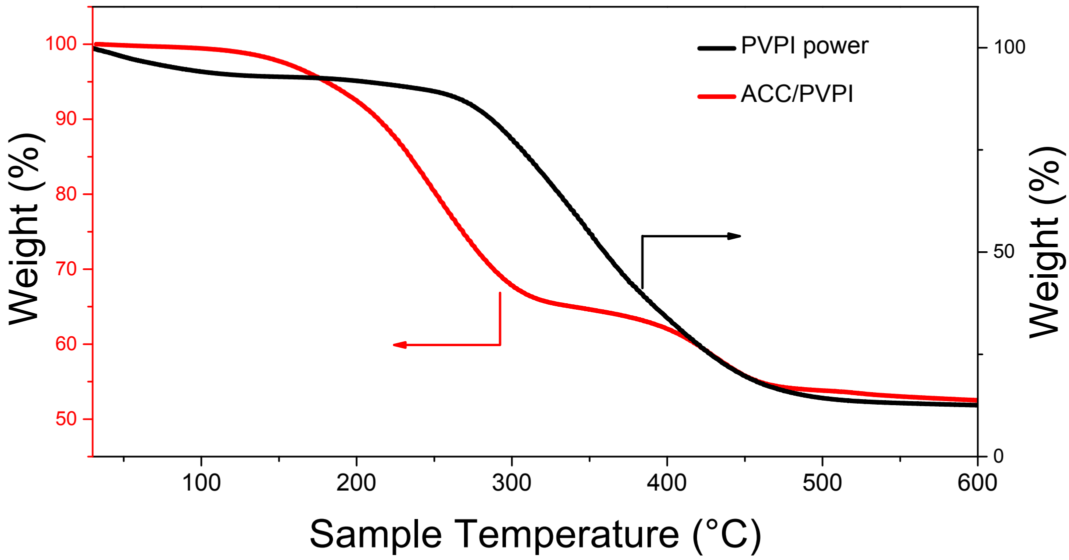

Figure S4. TG analysis of PVPI power and ACC/PVPI electrode.

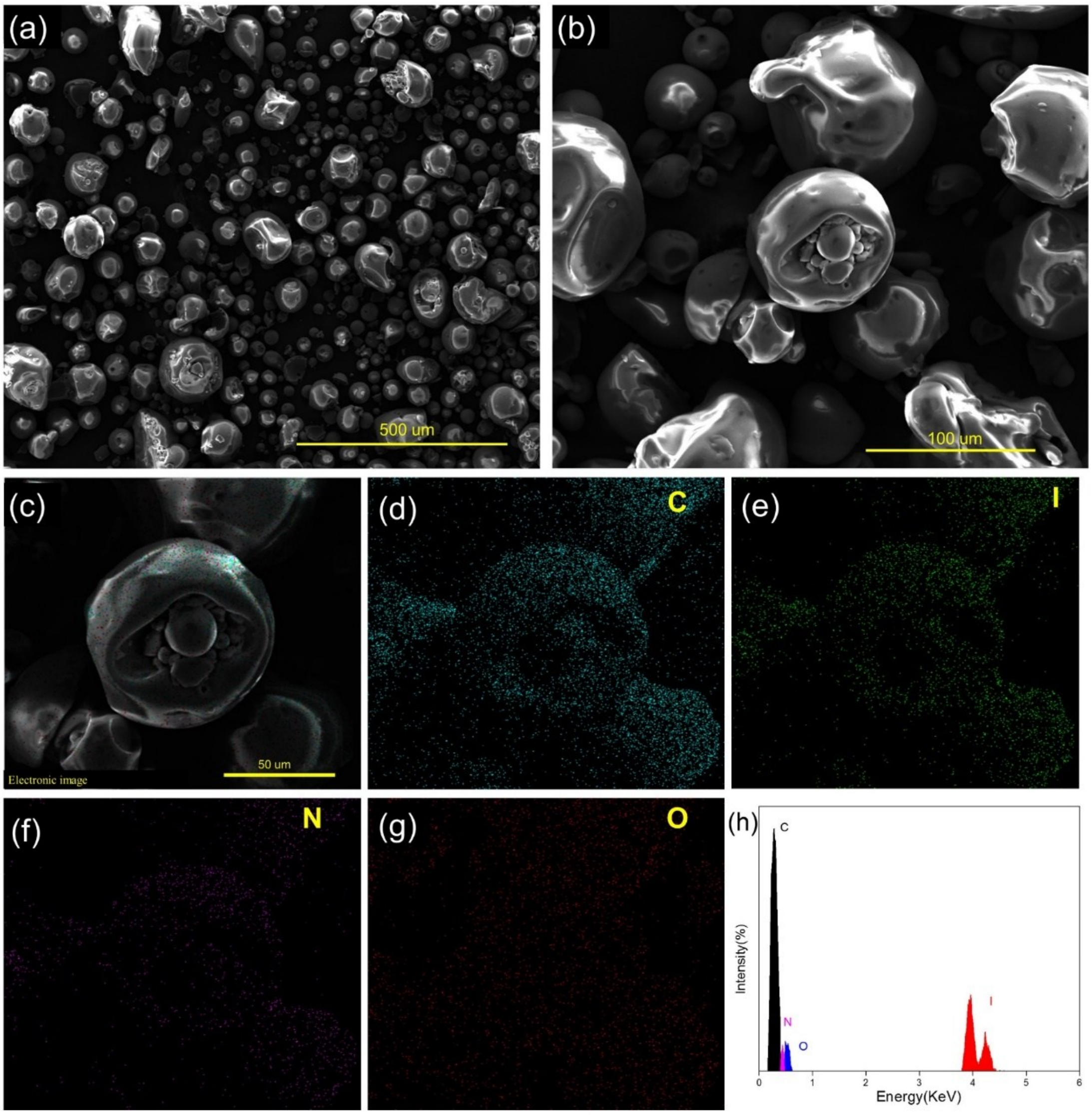

Figure S5. Characterization of the commercial PVPI. (a)-(b) SEM image of primary PVPI particles. (c) Electronic image of elemental mapping images. Elemental mapping images of the PVPI particles for carbon (d); iodine (e); nitrogen (f) and oxygen (g). (h) EDS of the PVPI particles.

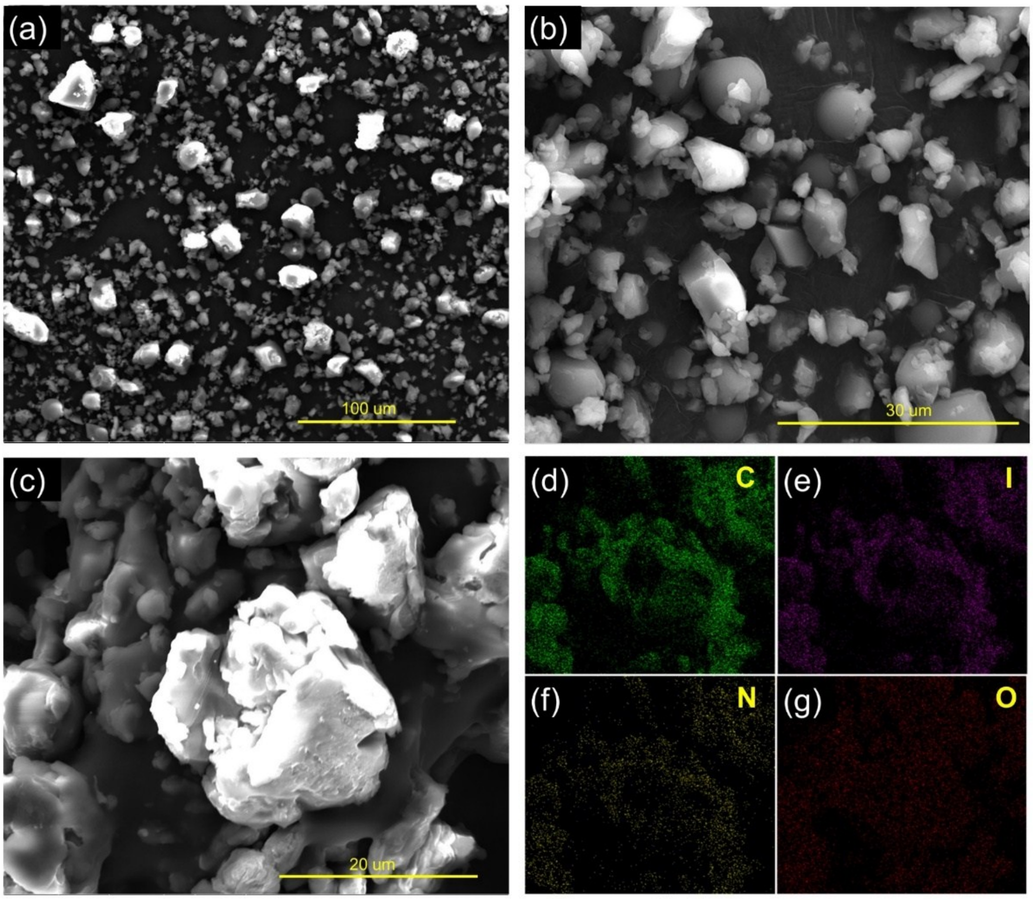

Figure S6. (a)-(c) SEM images of PVPI after ball milling. (d-g) the elemental mapping images of the ball-milled PVPI for carbon (d); iodine (e); nitrogen (f) and oxygen (g). After ball milling, the average size of PVPI particle decreased.

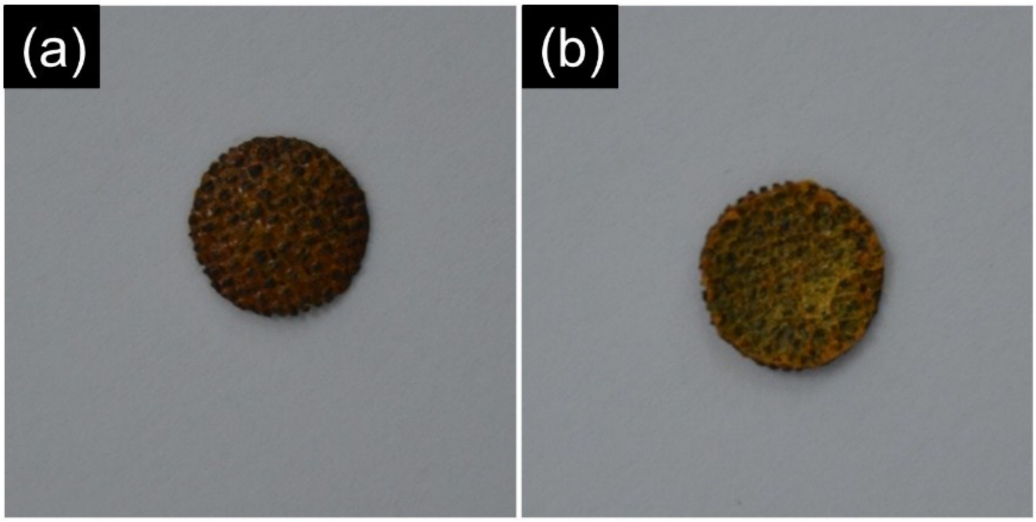

Figure S7. Optical photographs of ACC/PVPI after freeze-dry for 12 h. (a)-(b) pros and cons.

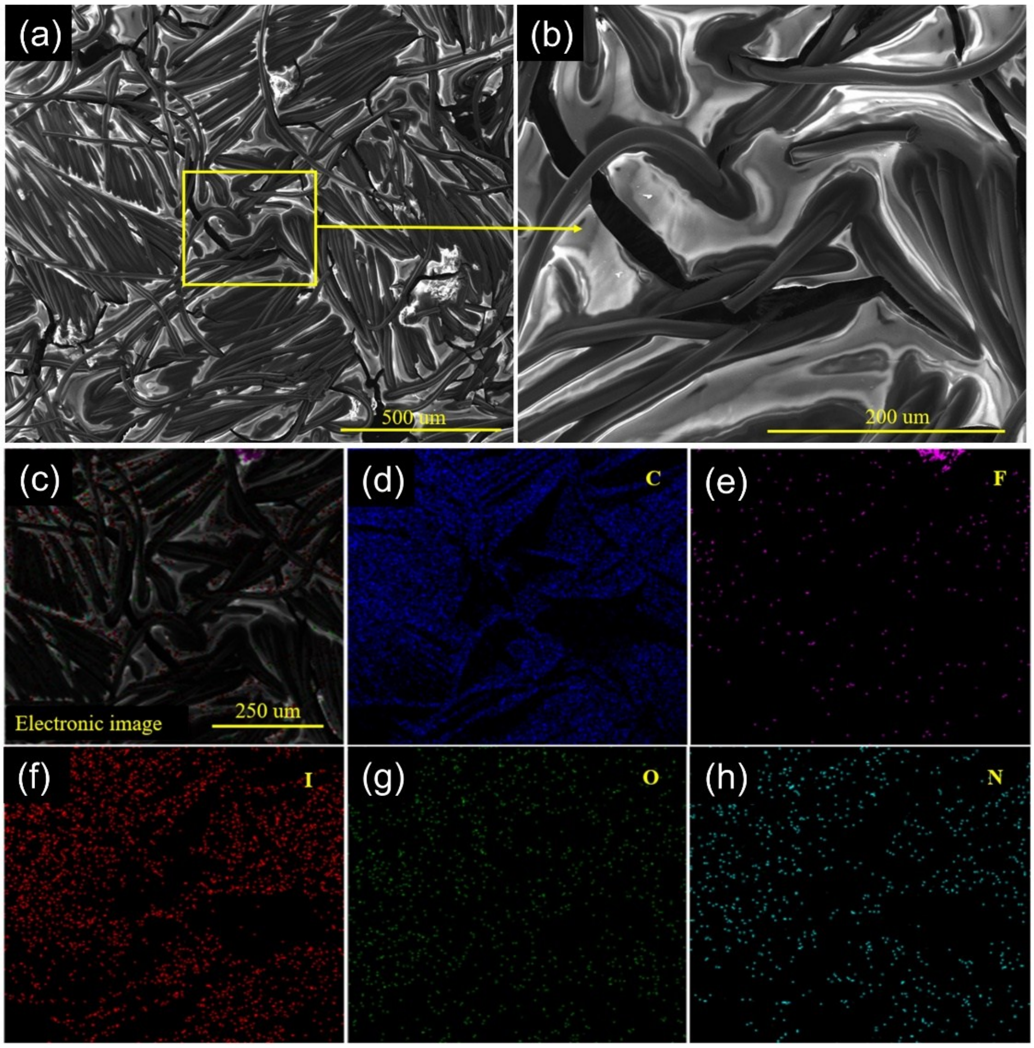

Figure S8. (a)-(b) SEM image of ACC/PVPI after freeze-dry. (c) Electronic image of elemental mapping images. (d)-(h)the elemental mapping images of ACC/PVPI after freeze-dry for carbon; fluorine; iodine; oxygen and nitrogen, respectively.

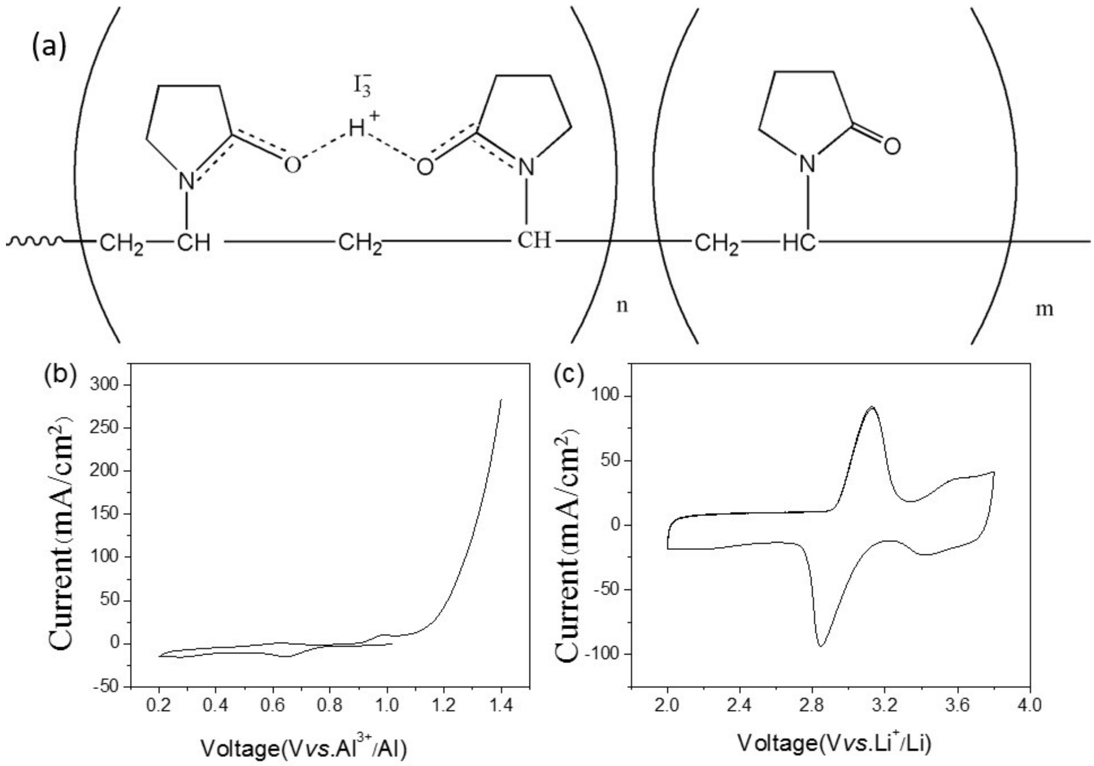

Figure S9. (a) The chemical formula of poly(vinylpyrrolidone)-iodine complex. (b)-(c) Wide range CV curves of the Al/I_2 and Li/I_2 cell with a scan rate of 0.1 mV/s.

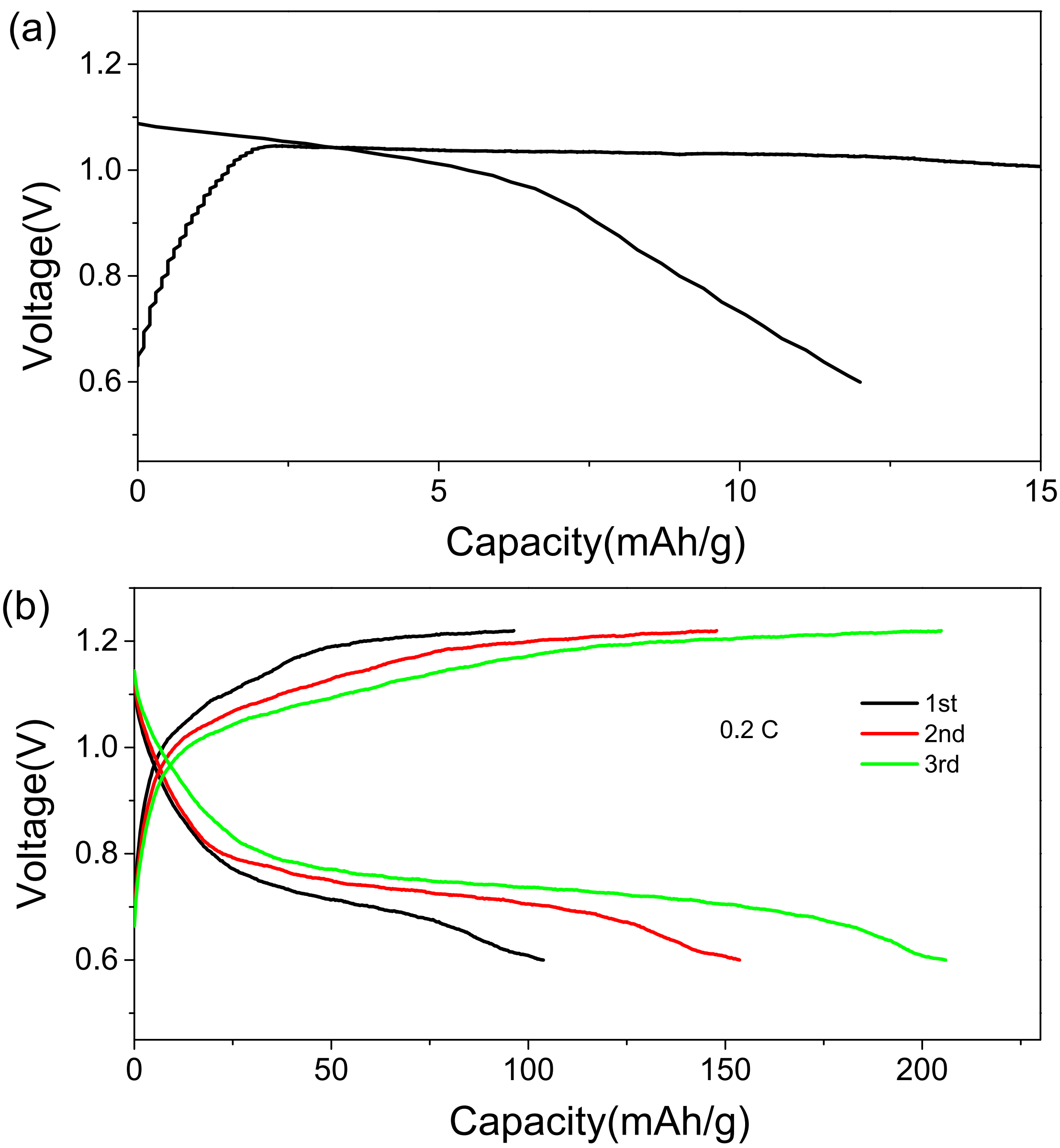

Figure S10. (a) Typical discharge/charge curves of the ACC/I_2 cathode. (b) Discharge and charge curves of the Al/I_2 battery at a constant current rate of 0.2 C based on ACC/PVPI cathode.

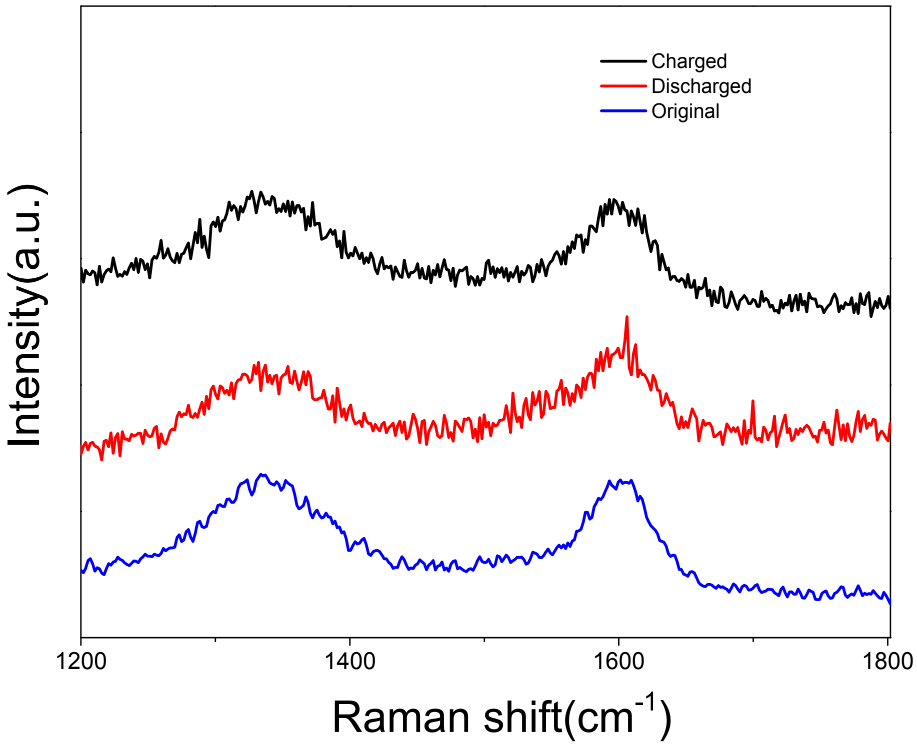

Figure S11. Raman spectra of ACC/PVPI cathode at different states in the wavelength range of 1200–1800 cm^{-1}.

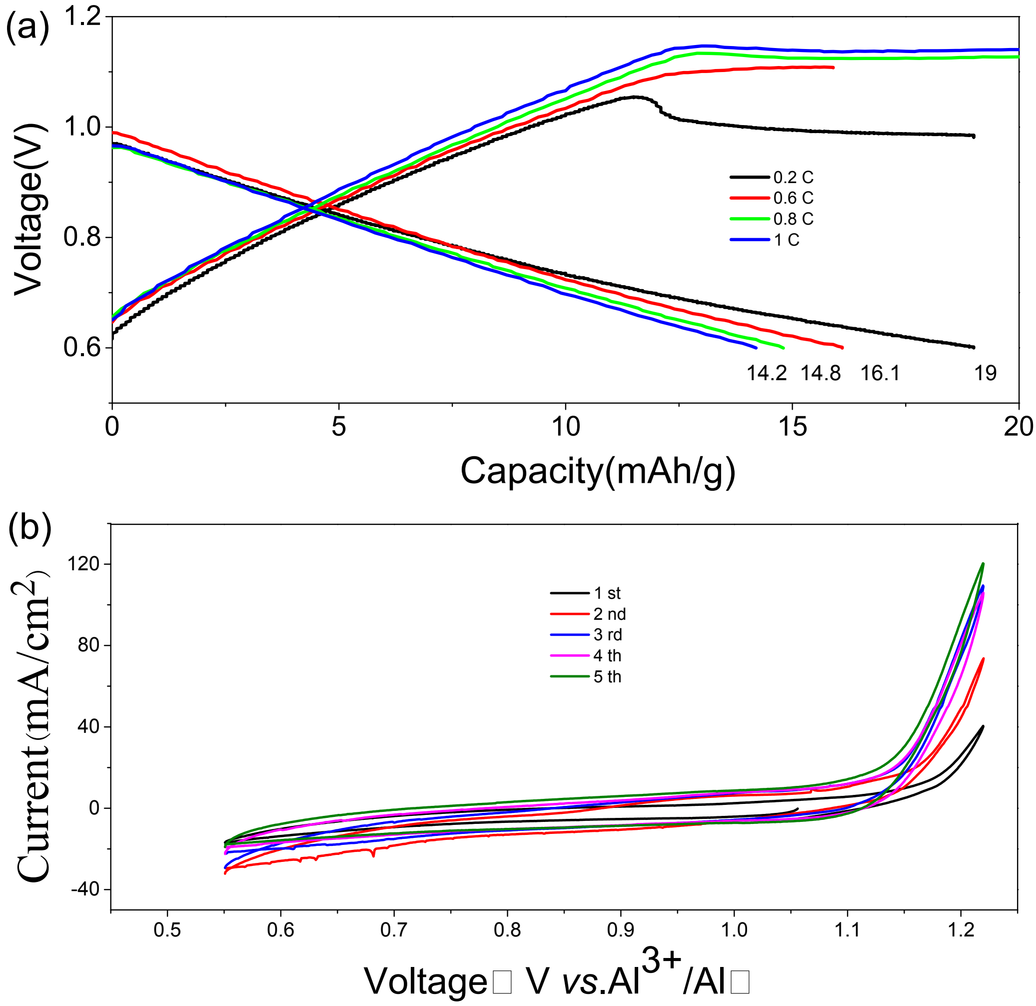

Figure S12. Electrochemical characterization of the blank active carbon cloth (ACC). (a) Discharge/charge curves of the ACC. (b) CV curves of the ACC with a scan rate of 0.1mV/s. The capacity is calculated based on the mass of ACC. This capacitive storage of ACC is about 15～20 mAh/g in different current rate. Note: in order to be compared with rate performance of the as-prepared ACC/PVPI, 1C=211mA/g, i.e. the theoretical capacity of iodine.

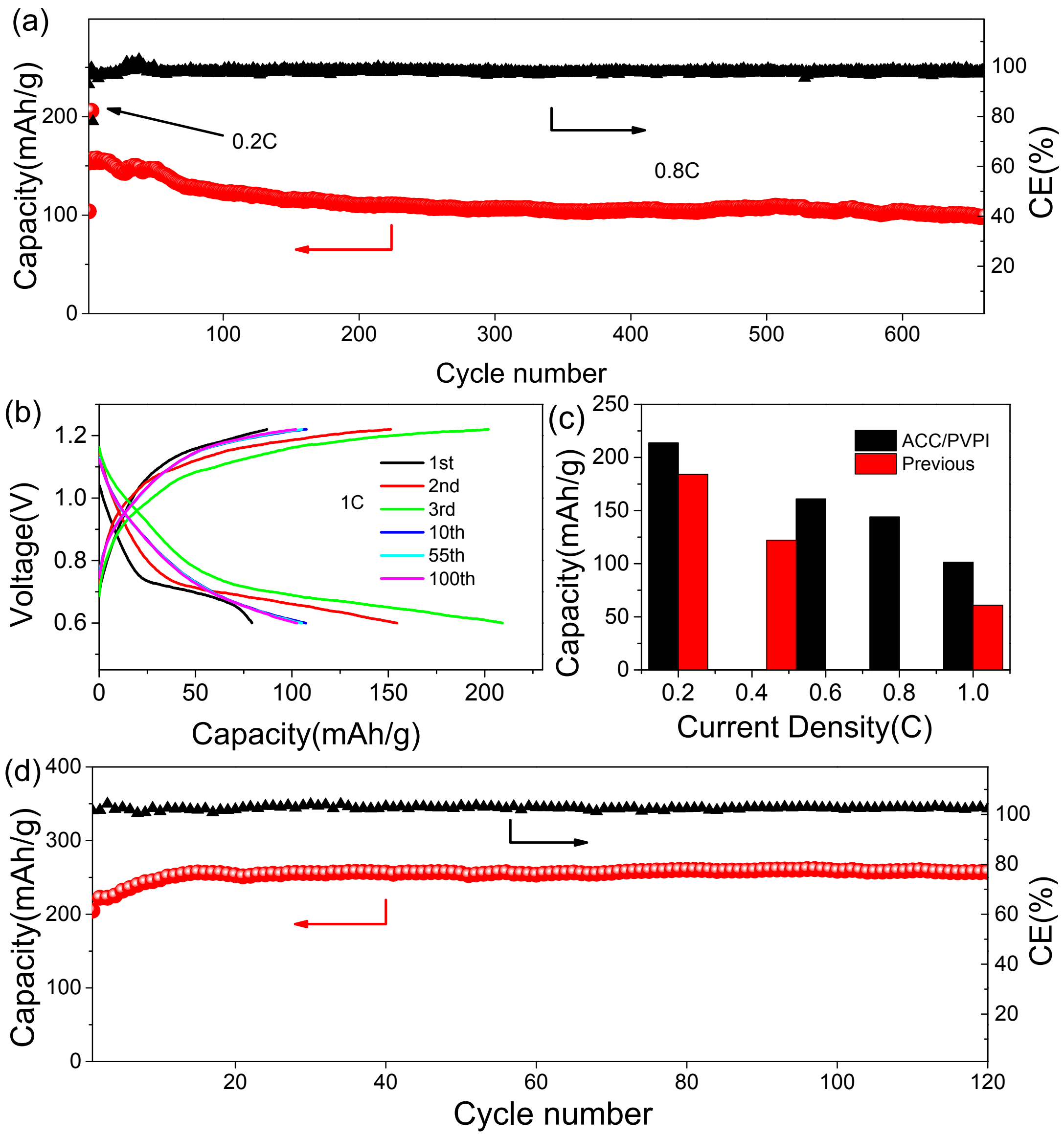

Figure S13. (a) Cycling performance of Al/I_2 battery at 0.8 C. (b) Typical galvanostatic charge/discharge curve of Al/I_2 battery at 1 C in certain cycles. (c) Comparison of rate performance with previous report. (d) Cycling performance of Li/I_2 battery at 0.2 C.

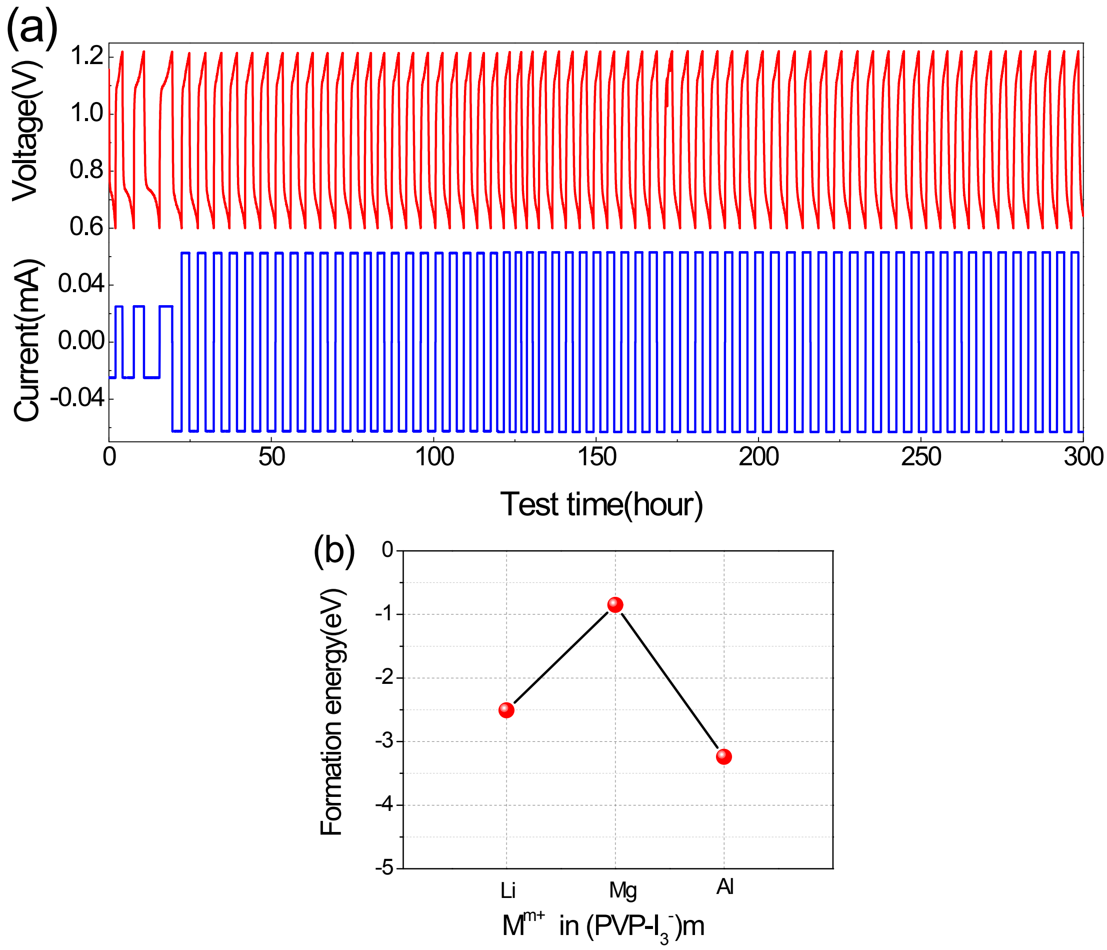

Figure S14. (a) Discharge/charge voltage and current profiles of the Al/I_2 battery in 300 h at 0.6 C. **(b)** Calculated formation energy of for different metal ions in $M^{m+}(PVP\text{-}I_3^-)m$ (M = Li, Mg, Al) products.

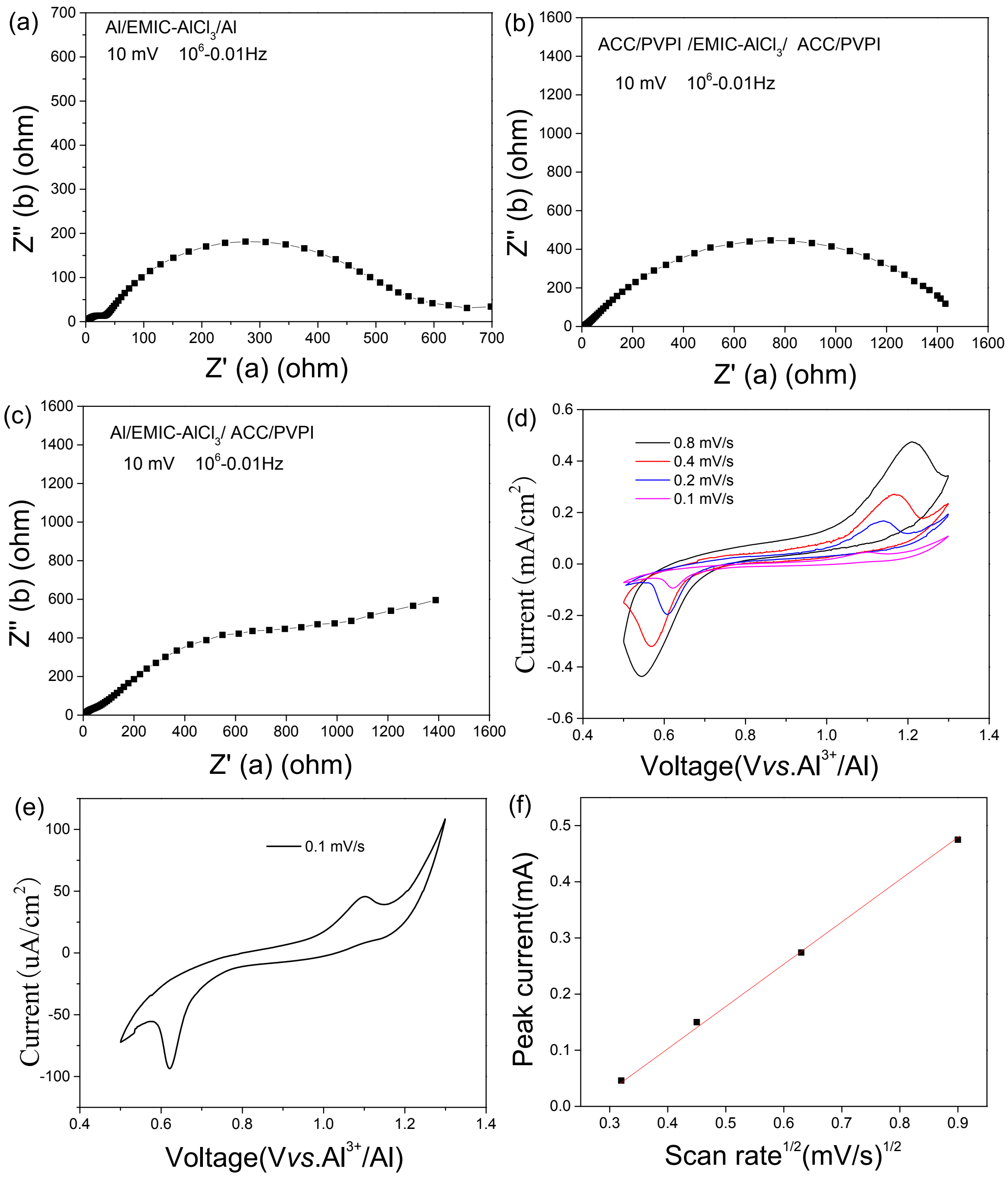

Figure S15. (a)-(c) Electrochemical Impedance Spectrum (EIS) of the anode electrode symmetrical cell, the cathode electrode symmetrical cell, Al/ ACC/PVPI battery, respectively. (d) CV curves of the as-prepared ACC/PVPI electrode at different scan rates. (e) Close up view of CV curves at 0.1 mV/s. (f) the relationship between the peak currents and scan rates.

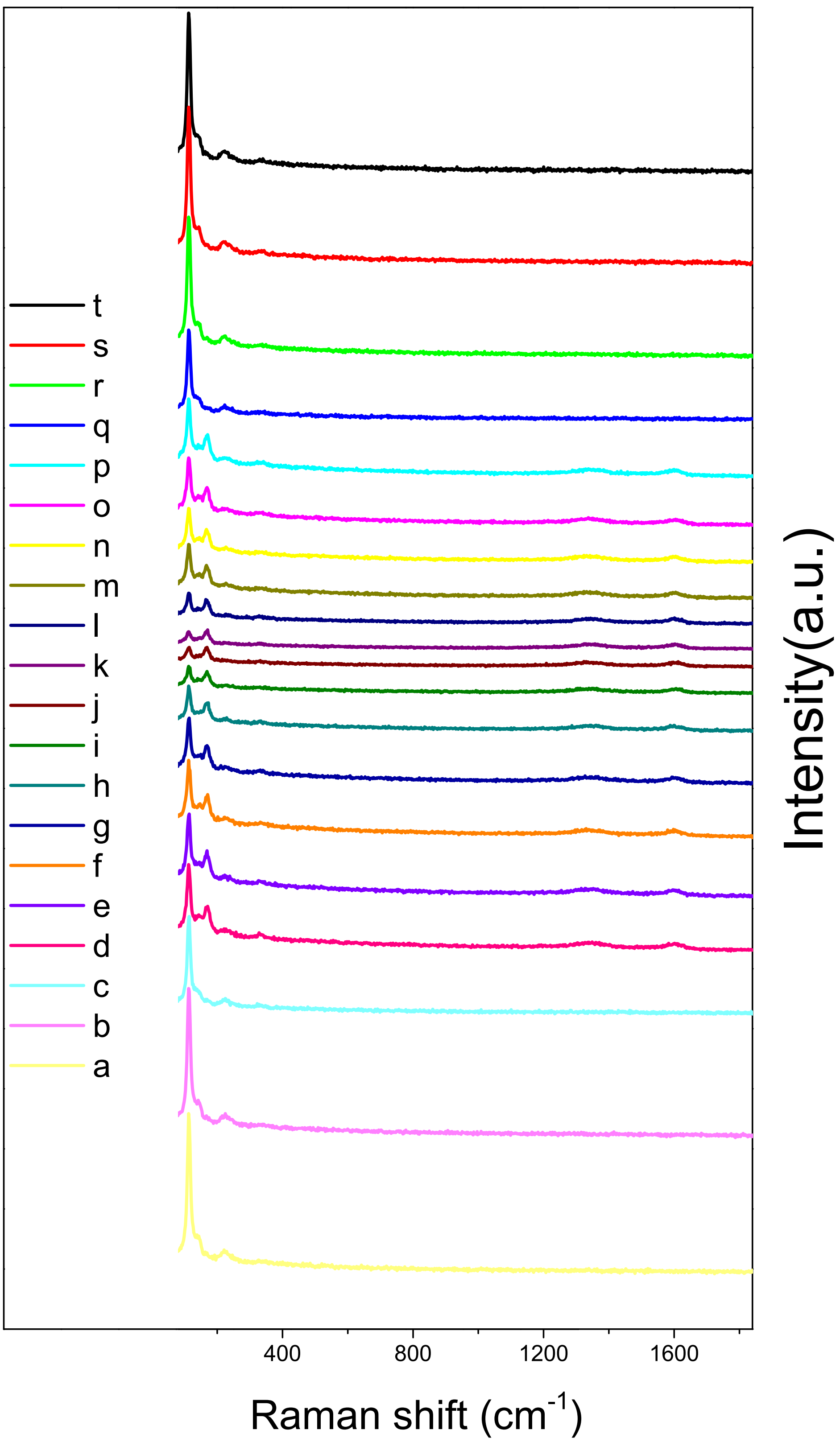

Figure S16.Raman of the corresponding point marked in Figure 4g in the wavelength range of 80–1840 cm^{-1}.

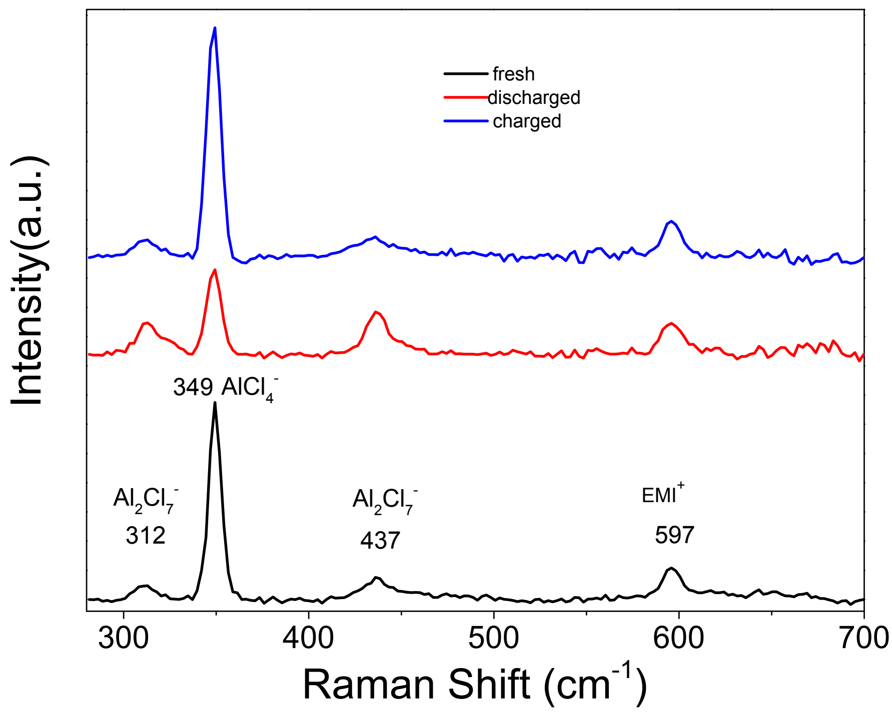

Figure S17. Raman spectra of the $AlCl_3$/[EMIm]Cl ionic liquids electrolytes in different states with a molar ratio of $AlCl_3$/[EMIm]Cl=1.3.

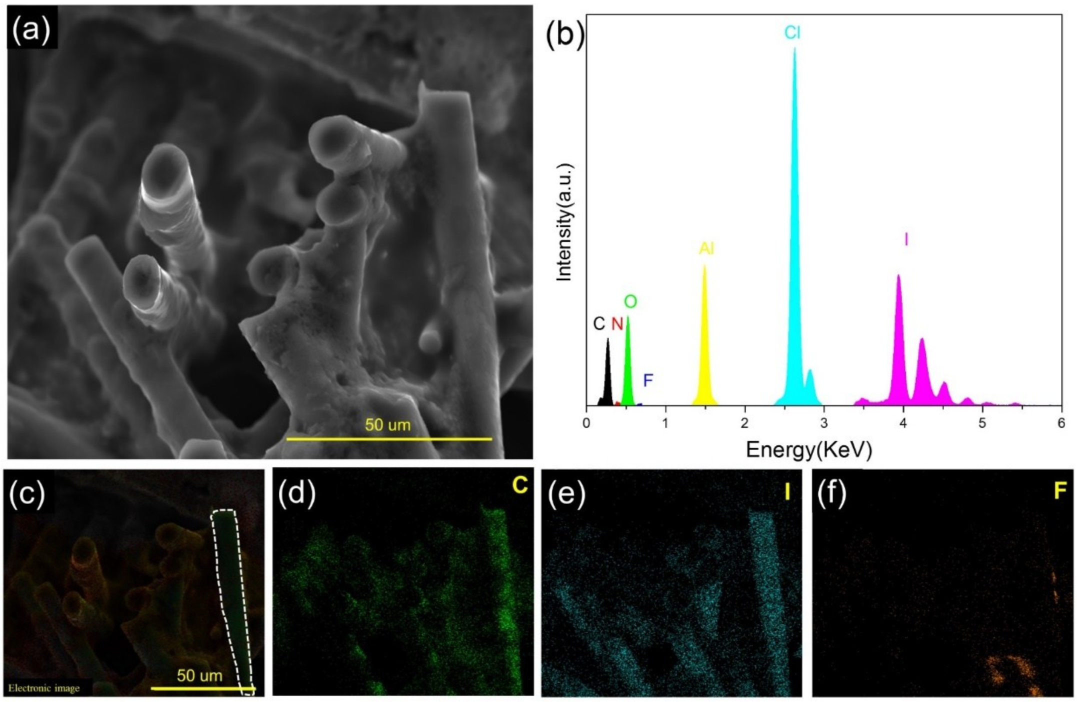

Figure S18. (a) SEM image of ACC/PVPI after fully charged. (b) EDS of the ACC/ PVPI after fully charged. (c) Electronic image of elemental mapping images. (d)-(f)the elemental mapping images of ACC/PVPI after fully charged for carbon, iodine and fluorine, respectively.

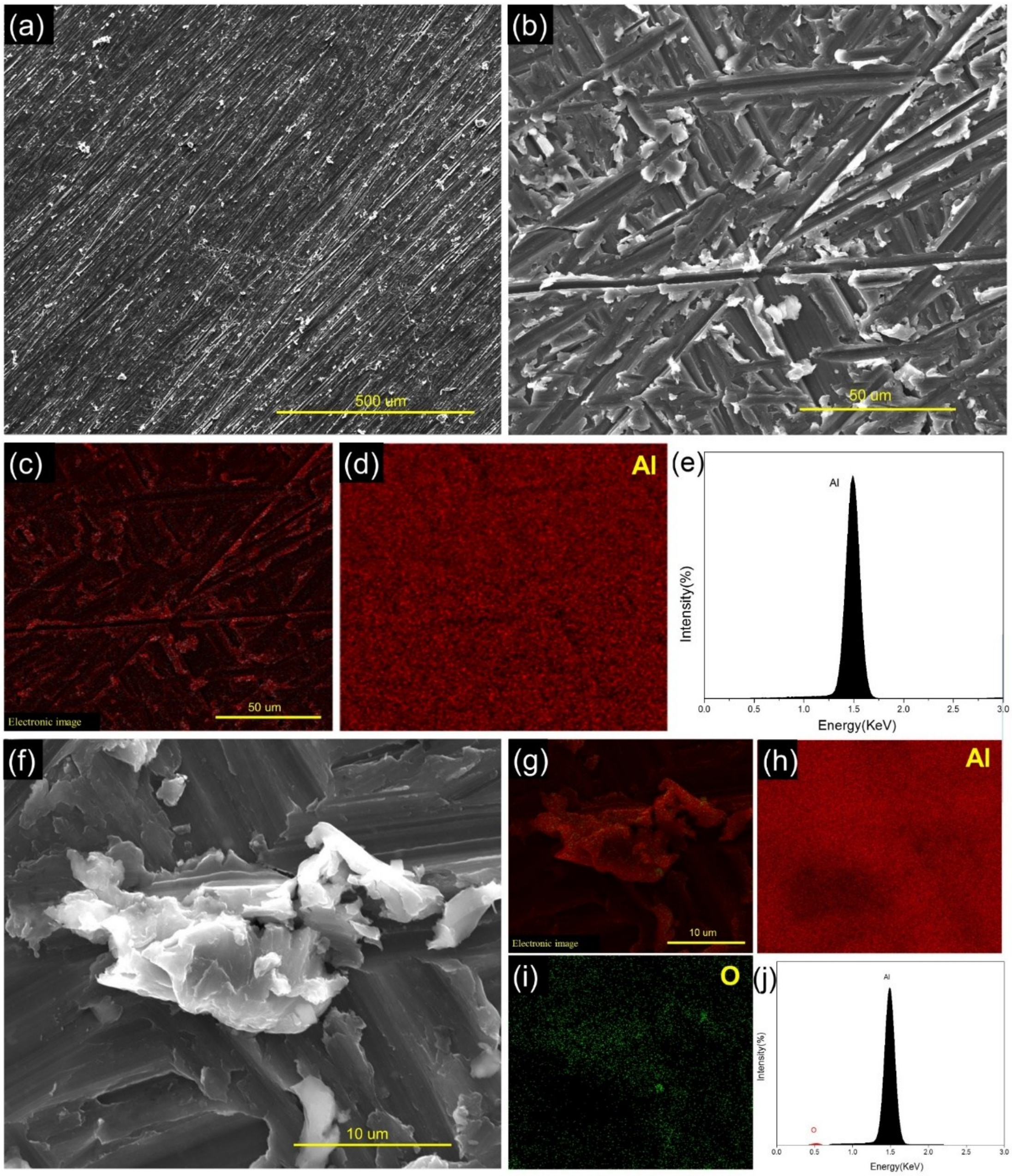

Figure S19. SEM images of Al anode before discharge/charge cycling. (a)-(b) SEM images of Al anode. (c) Electronic image of elemental mapping images. (d) the elemental mapping images of the Al anode for aluminum. (e) EDS of the Al anode and (f)-(j) another region characterization. Two different regions characterization results confirm that some aluminum oxide still exist on the surface of Al anode.

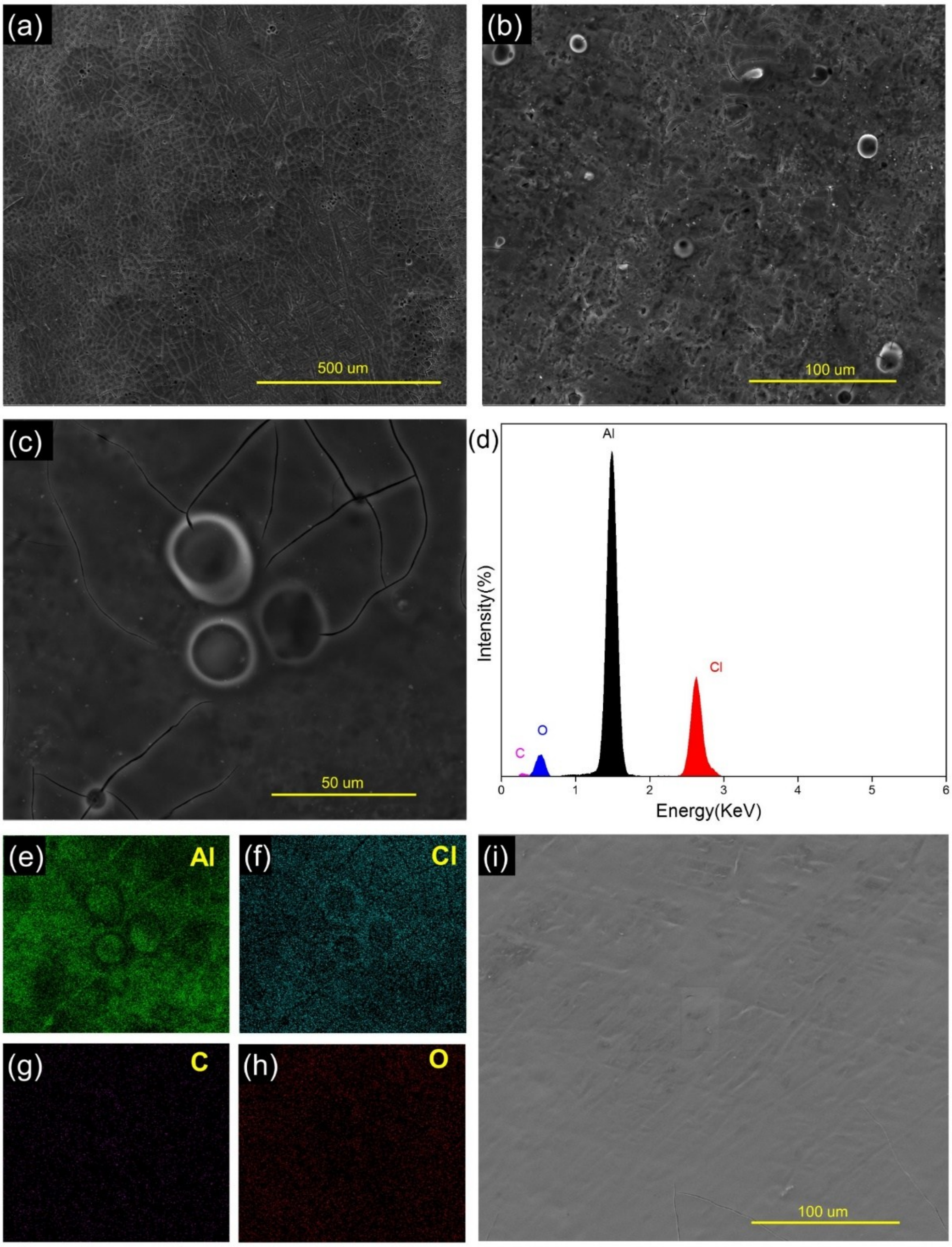

Figure S20. SEM images of Al anode after fully discharged and charged. (a)-(c) SEM images of Al anode after fully discharged. (d) EDS of the Al anode after fully discharged. (e)-(h) The elemental mapping images of the fully discharged Al anode for aluminum, chlorine, carbon and oxygen. (i) SEM images of Al anode after fully charged, indicating the dendrite free of Al during the deposition/stripping.

References

1. M. C. Lin, M. Gong, B. G. Lu, Y. P. Wu, D. Y. Wang, M. Y. Guan, M. Angell, C. X. Chen, J. Yang, B. J. Hwang and H. J. Dai, *Nature*, 2015, **520**, 325-328.
2. S. Wang, Z. Yu, J. Tu, J. Wang, D. Tian, Y. Liu and S. Jiao, *Advanced Energy Materials*, 2016, **6**, 1600137-1600146.
3. H. Wang, S. Gu, Y. Bai, S. Chen, N. Zhu, C. Wu and F. Wu, *J. Mater. Chem. A*, 2015, **3**, 22677-22686.
4. N. Jayaprakash, S. K. Das and L. A. Archer, *Chemical Communications*, 2011, **47**, 12610-12612.
5. W. Wang, B. Jiang, W. Xiong, H. Sun, Z. Lin, L. Hu, J. Tu, J. Hou, H. Zhu and S. Jiao, *Sci Rep*, 2013, **3**, 3383.
6. Y. P. Wu, M. Gong, M. C. Lin, C. Z. Yuan, M. Angell, L. Huang, D. Y. Wang, X. D. Zhang, J. Yang, B. J. Hwang and H. J. Dai, *Advanced Materials*, 2016, **28**, 9218-+.
7. S. Jiao, H. Lei, J. Tu, J. Zhu, J. Wang and X. Mao, *Carbon*, 2016, **109**, 276-281.
8. J. V. Rani, V. Kanakaiah, T. Dadmal, M. S. Rao and S. Bhavanarushi, *Journal of the Electrochemical Society*, 2013, **160**, A1781-A1784.
9. N. S. Hudak, *Journal of Physical Chemistry C*, 2014, **118**, 5203-5215.
10. Y. Hu, B. Luo, D. Ye, X. Zhu, M. Lyu and L. Wang, *Adv Mater*, 2017.
11. S. Wang, S. Q. Jiao, J. X. Wang, H. S. Chen, D. H. Tian, H. P. Lei and D. N. Fang, *Acs Nano*, 2017, **11**, 469-477.
12. N. P. Stadie, S. T. Wang, K. V. Kraychyk and M. V. Kovalenko, *Acs Nano*, 2017, **11**, 1911-1919.
13. L. X. Geng, J. P. Scheifers, C. Y. Fu, J. Zhang, B. P. T. Fokwa and J. C. Guo, *Acs Applied Materials & Interfaces*, 2017, **9**, 21251-21257.
14. L. X. Geng, G. C. Lv, X. B. Xing and J. C. Guo, *Chemistry of Materials*, 2015, **27**, 4926-4929.